JOURNAL OF BIOMOLECULAR STRUCTURE AND DYNAMICS
https://doi.org/10.1080/07391102.2021.1887763

Identification of the binding interactions of some novel antiviral compounds against Nsp1 protein from SARS-CoV-2 (COVID-19) through high throughput screening

Nilkanta Chowdhury and Angshuman Bagchi

Department of Biochemistry and Biophysics, University of Kalyani, Kalyani, West Bengal, India

Communicated by Ramaswamy H. Sarma

ABSTRACT

The SARS-CoV-2 pandemic has become a global threat. It has become very difficult to control the spreading of the virus. The virus is a RNA virus and the virulence of the virus is mediated by three virulence causing proteins, viz., Nsp1, Nsp3c and ORF7. So far the drug designing endeavors against the virus have been being targeted towards the spike protein which is responsible for the entry of the virus inside human host as well as the RNA dependent RNA polymerase. However, no effective treatment against the virus has so far been developed. In the present situation, an attempt has been made to target the virulence protein factor Nsp1 which binds to the 40S ribosomal subunit of the human host. We tried to target the Nsp1 by in-silico virtual screening of ligand libraries. We built the three dimensional structure of Nsp1 and used the structure to screen the ChEMBL drug library. We used molecular docking simulations of the top6 screened ligands with Nsp1 and subjected the liagnd-Nsp1 complexes to molecular dynamics simulations to analyze the behaviors of the ligands in a virtual cell. From our analysis we could predict that the ligands bearing the ChEMBL identifiers, CHEMBL1096281, CHEMBL2022920, CHEMBL175656, had the best binding affinity values with Nsp1. Therefore, these ligand molecules may be tested in wet-lab for further analysis. This is the first report to target the virulence factor Nsp1 from SARS-CoV-2.

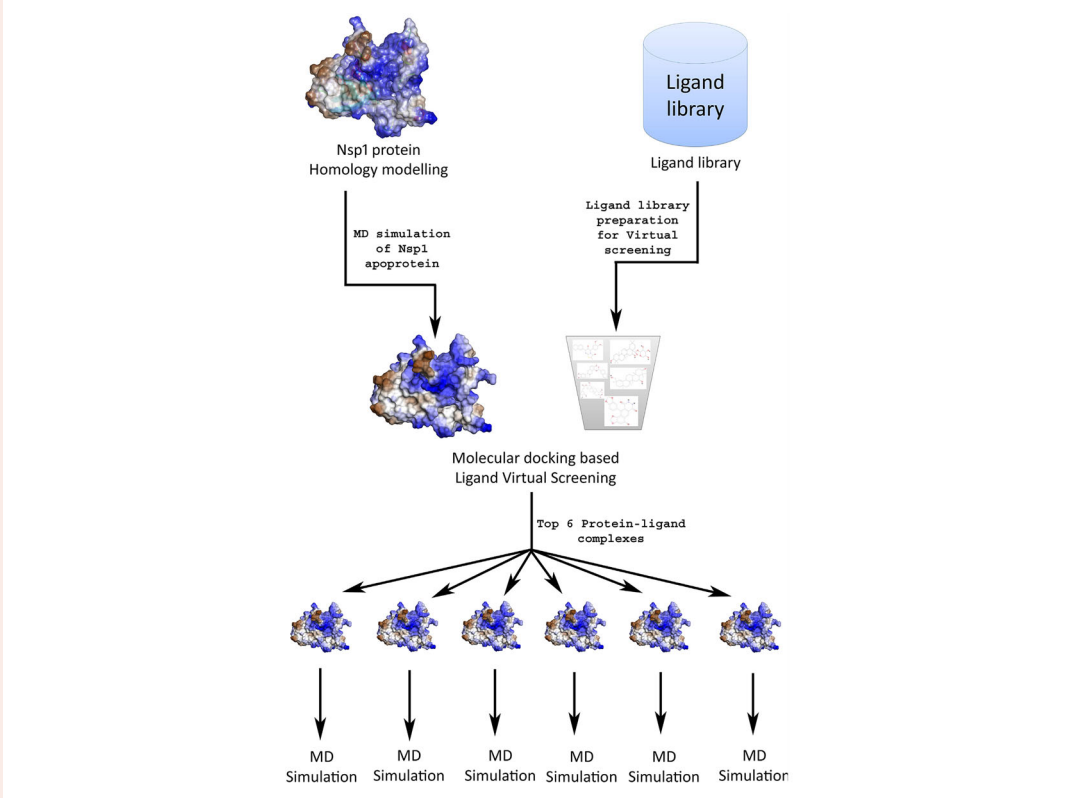

ARTICLE HISTORY
Received 20 October 2020
Accepted 4 February 2021

KEYWORDS
SARS-CoV-2; virulence factors; Nsp1; drug designing; virtual screening; docking; molecular dynamics simulations

CONTACT Angshuman Bagchi nilkanta@klyuniv.ac.in, angshu@klyuniv.ac.in, angshumanb@gmail.com Department of Biochemistry and Biophysics, University of Kalyani, Kalyani, West Bengal 741235, India

Supplemental data for this article can be accessed online at https://doi.org/10.1080/07391102.2021.1887763.

1. Introduction

The latest outbreak of the deadly coronavirus during the later part of 2019 has become a global threat to the survival of the mankind. The virus is claiming thousands of lives everyday worldwide. The commonest symptoms of the viral infection include severe respiratory troubles with subsequent fever. Therefore, the International Committee of Viral Taxonomy has named the virus as the severe acute respiratory syndrome coronavirus 2 (SARS-CoV-2 or 2019-nCOV). Such is the severity of the viral infection that the World Health Organization (WHO) coined the pandemic as COVID-19. Coronaviruses are commonly divided into four main genera, such as, Alphacoronavirus, Betacoronavirus, Gammacoronavirus and Deltacoronavirus (Fung et al., 2020). The SARS-CoV-2 is a member of the Betacoronavirus family. The virus is a single stranded RNA virus with a glycoprotein envelope. The virus contains a polycistronic genome which codes for a number of non-structural proteins (represented as nsp1 to nsp16 merged together as a poly-protein ORF1) along-with structural and other accessory proteins (Sahin, 2020). Once the SARS-CoV-2 infects a human host, a viral protease called Papain-like proteinase or 3 C-like protease (3CLpro) cleaves off the poly-protein to release three virulence factors, Nsp1, Nsp3c and ORF7. These virulence factors would help the onset of viral infection cycle by shutting down the innate immune system of the human host such that the virus would no longer be diagnosed by the immune system of the human host (Chen Cao et al., 2020). One of the virulence factors, Nsp1, binds to the 40S ribosomal subunit of the human host and inactivates the translational activity of 40 s ribosome. The Nsp1-40S-ribosome complex modifies the 5′-region of capped mRNA template of the human host and makes the mRNA incompetent for translation. Nsp1 also leads to the degradation of host cell mRNAs (Kamitani et al., 2009). It was observed that any alteration in the amino acid sequence in the region spanning the amino acids 160 to 173 of Nsp1 led to the inactivation of the protein (Narayanan et al., 2008). Furthermore, it has also been reported by in vitro alanine mutagenesis analysis that the two positively charged amino acids residues, viz., Lys164 and His165 are the key residues of Nsp1 for binding the 40S ribosomal subunit (Kamitani et al., 2009).

In short, Nsp1 degrades the antiviral immune response of the human host and would therefore play the most vital role in the replication of the virus inside the human host. The vital role of the Nsp1 protein has made it an important target for the development of antiviral therapy. Unfortunately, there are no antiviral drugs available till date which could be used against Nsp1 from the newly identified SARS-CoV-2 (Wu, 2020). Under such circumstances, an attempt has been made to propose the structures and properties of potential new molecules with proven anti-viral properties that could target the Nsp1 protein from the newly identified SARS-CoV-2. We modeled the three dimensional structure of the Nsp1 and used the structure to screen ChEMBL library (Gaulton et al., 2017) and NCI ligand library (Shiryaev et al., 2011), to find suitable drug like compounds by the method of virtual screening. We targeted the patch of amino acid residues spanning the region 160 to 173 on the surface of the Nsp1 for ligand screening. The top 6 compounds obtained from the virtual screening method were used to dock with Nsp1 and the real life behaviors of the docked complexes were analyzed by molecular dynamics simulations. From our analysis, we could filter out certain specific anti-viral compounds which might be tested in wet-lab. So far, this is the only report that provides the molecular insight into targeting the Nsp1 from SARS-CoV-2. Our main aim to target the Nsp1 was that the protein is a relatively less targeted one. One of the main difficulties in the development of new anti-viral drugs is to obtain specific lead-like compounds from the repositories of millions of compounds. We hope that our work would help in identifying potential anti-viral therapies against SARS-CoV-2 by narrowing down the anti-viral target molecules from thousands of compounds available in different databases. The anti-viral compounds predicted by our analysis would certainly expedite the drug designing endeavor and therefore would facilitate the invention of new therapies to prevent the SARS-CoV-2 infection.

2. Materials and methods

2.1. Sequence analysis and molecular modeling of Nsp1 from SARS-CoV-2

The amino acid sequence of Nsp1 from SARS-CoV-2 was retrieved from NCBI bearing the accession number YP_009725297.1 [https://www.ncbi.nlm.nih.gov/protein/1802476805]. We used the amino acid sequence to calculate certain physico-chemical characteristics, like the pI, the molecular weight, the instability index of the protein using the tools in ExPASy server (Gasteiger et al., 2003). There is no crystal structure of Nsp1 (Search date: 30/03/2020) available in RCSB PDB database. In order to perform the ligand binding experiments with Nsp1, we built a full-chain three dimensional model of the Nsp1 using Phyre2 server (Kelley et al., 2015) (Figure 1).

The stereo-chemical qualities of the modeled protein were checked by Verify3D (Eisenberg et al., 1997), ProSA (Wiederstein & Sippl, 2007), PROCHECK (Laskowski et al., 1993) and Ramachandran plots were drawn. The Verify3D and ProSA scores were found to be 85.56 & −6.14 respectively which would reflect a good model quality (Supplementary Figure 1). Furthermore, none of the amino acid residues were found to be present in the disallowed regions of the Ramachandran plot. The selected model of Nsp1 from Phyre2 was then subjected to molecular dynamics (MD) simulation in GROMACS (Van Der Spoel et al., 2005) for 120 nanoseconds (ns) to check its real life behavior inside the cell. We used the same protocol for MD simulation as mentioned in the section 2.3. However, we observed that Nsp1 had attained structural stability after a simulation run of 60 ns as expressed by the Root Mean Squared Deviation (RMSD) of the Cα backbone atoms of Nsp1 (Figure 2).

A representative structure from this MD simulation run was generated using clustering method in GROMACS. We again checked the stereo-chemical qualities of this representative structure obtained from the MD simulation. Now, the

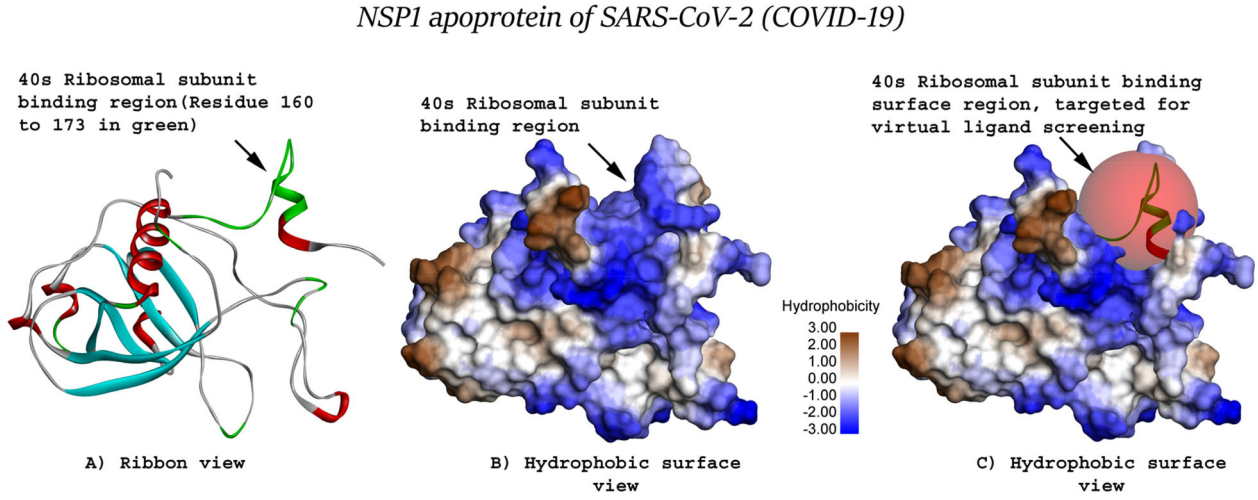

Figure 1. Nsp1 apoprotein. A. Ribbon representation of the Nsp1. The helices are shown in red; the sheets are presented in cyan. The remaining part is loop. The 40S ribosomal subunit binding region is presented in green. B. The surface representation of the Nsp1 protein. The 40S ribosomal subunit binding region is blue representing a positively charged region. The protein has a hydrophobic patch. C. The 40S ribosomal subunit binding surface region targeted for virtual screening of ligand libraries.

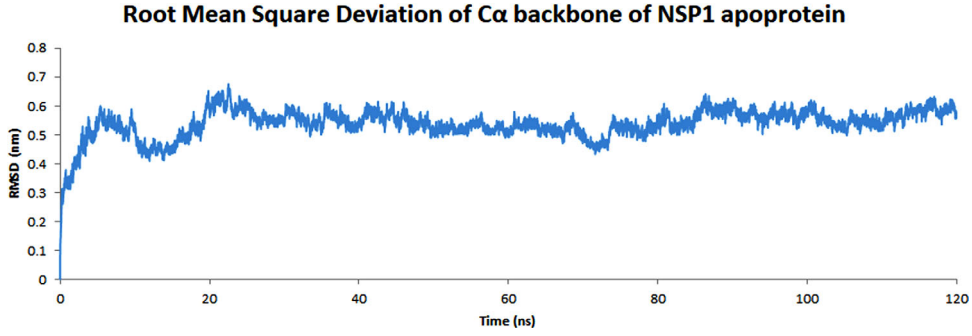

Figure 2. RMSD of the Cα backbone atoms of the Nsp1 during the course of MD simulation. The plot was found to be linear around 100 ns. Therefore, the protein may be considered to attain a stable conformation with less structural fluctuations around the 100 ns of the simulation run.

Verify3D and ProSA scores were found to be 93.89 & −6.56 respectively which would reflect an improvement in the quality of the structure of Nsp1 after MD simulation (Supplementary Figure 2). This representative structure of the Nsp1 protein was used for virtual screening experiments.

2.2. Virtual screenings of molecular libraries

For virtual screening experiments, we used the collection of antiviral compounds present in ChEMBL database containing 1391 structures. In order to perform an exhaustive search to find the suitable ligands, we screened the NCI ligand database containing 16,283 potential anti-viral compounds. The structural optimizations of the compounds were performed with the help of 'prepare ligand' protocol in Discovery Studio (DS). The atomic charges and protonation states of the selected ligand molecules were standardized for common functional groups present in the structures of these screened compounds using the 'prepare ligand' module in DS. Finally, a library of three dimensional coordinates of the antiviral compounds was generated in DS. We then used this ligand library for virtual screening using AutoDock vina (Cosconati et al., 2010; Jiménez-Alberto et al., 2020). We performed site specific docking, using the 40 s ribosomal subunit binding site of the Nsp1 as the docking target. We performed 10 GA run for each docking simulation.

In total, we did the virtual screenings of 17,674 ligands (1391 fom ChEMBL + 16283 from NCI) obtained from the two different ligand databases in two separate virtual screening runs. From the virtual screening results, we selected the top six ligands obtained from each run of the virtual screening process.

The top six ligands, obtained from ChEMBL database after virtual screenings, were CHEMBL1096281 (Mohamed et al., 2010), CHEMBL2386944 (Yu et al., 2013), CHEMBL1761178 (Bodiwala et al., 2011), CHEMBL2022920 (Osorio et al., 2012), CHEMBL464486 (De Tommasi et al., 1992), and CHEMBL175656 (Yeo et al., 2005) (Figure 3). The binding interaction energy values of these top six compounds calculated using AutoDock were, −9.0 (kcal/mol), −8.8 (kcal/mol), −8.7 (kcal/mol), −8.5 (kcal/mol), −8.4 (kcal/mol) and −8.4 (kcal/mol) respectively.

Top six ligands, obtained from NCI database after virtual screenings, were NCI_232490, NCI_332061, NCI_301755, NCI_657577, NCI_724037, and NCI_215618. The binding interaction energy values of these top six compounds calculated using AutoDock were, −8.2 (kcal/mol), −7.9 (kcal/mol), −7.9 (kcal/mol), −7.9 (kcal/mol), −7.8 (kcal/mol) and −7.8 (kcal/mol) respectively.

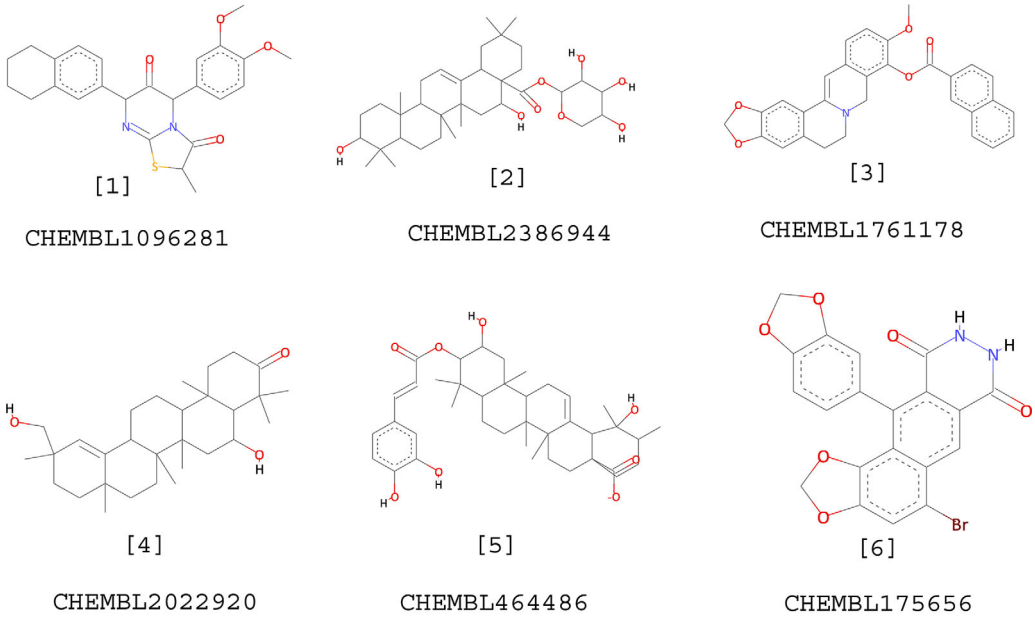

Figure 3. Description of the top 6 ligand molecules from virtual screening of ChEMBL.

From the binding interaction energy values, it could be safely concluded that the ligands obtained from ChEMBL had better binding affinities with Nsp1 than the ligands from NCI database. Therefore, we chose the top six ligands obtained from ChEMBL database for further analyses. The ADME properties of these selected compounds are presented in Supplementary Table 1.

2.3. Molecular dynamics (MD) simulation study of the Nsp1-ligand complexes

We used the three dimensional coordinates of the atoms of Nsp1 bound to the six different ligand molecules as obtained from the aforementioned virtual screening methods. As a control, we performed another MD simulation of free Nsp1 protein (Nsp1 apoprotein), which was used in virtual screening. For MD simulation we used GROMACS 5.1.5 tool. We used the SPC/E (Berendsen et al., 1987) water model to dissolve the Nsp1-ligand complexes in a water box keeping a minimum distance between the center of protein-ligand complex and box edge at 10 Å with CHARMM27 force field (Liang et al., 2020). Charge neutralizations of the protein-ligand complexes were carried out using requisite numbers of Cl^- and Na^+ ions. LINCS algorithm was used for constraining the bond lengths and bond angles (Hess et al., 1997). All the systems were energy minimized using steepest descent algorithm to remove any unwanted steric clashes. The minimization process was continued until the maximum force would reach 1000 kJ/mol/nm. The energy-minimized systems were equilibrated as per NVT followed by NPT simulation protocols for 100 picoseconds (ps) using periodic boundary conditions. The long range electrostatic interactions were calculated using Particle Mesh Ewald method (Sagui & Darden, 1999). The temperatures of the systems were kept at 310 K and were maintained by V-rescale, which is a modified Berendsen thermostat. Simultaneously, a constant pressure of 1 bar was maintained for all the systems by Parrinello-Rahman pressure coupling method. After this equilibration, all the systems were subjected to molecular dynamics run for 70 ns and the MD trajectory frames were saved after every 2ps. The MD trajectory frames were analyzed by GROMACS tool to calculate

a. the RMSD of the Cα backbone atoms of Nsp1 and the ligands,
b. the Root Mean Squared Fluctuations (RMSFs) of the atoms of the Nsp1 protein,
c. the distance between the ligand and the key amino acid residues, Lys164 and His165, on the protein surface.

We also performed clustering analysis using the tool g_cluster in GROMACS tool to determine the protein conformational diversities during the course of MD simulations.

2.4. MM/PBSA calculation

The binding free energy values for each protein ligand complexes were calculated using MM/PBSA method based on the final structures derived from the last 20 ns of MD simulation runs, using bootstrap analysis. MM/PBSA calculates the free energy changes of the binding interactions as:

$$\Delta G_{Bind} = G_{Complex} - (G_{Protein} + G_{Ligand})$$

$\boldsymbol{\Delta G_{Bind} = G_{Complex} - (G_{Protein} + G_{Ligand})}$

$\boldsymbol{\Delta G_{Bind}}$ = Change in free energy value of the binding of the ligand with the target protein receptor.

$\boldsymbol{G_{Complex}}$ = Free energy of the complex of target protein receptor bound to the ligand

$G_{Protein}$ = Free energy of the target protein receptor only
G_{Ligand} = Free energy of the ligand only

3. Results

3.1. Three dimensional structure of Nsp1 and other physico-chemical properties

The Nsp1 is a 180 amino acid residue long protein. The protein is made up of helices and strands joined by loops (Figure 1). The calculated molecular weight of the protein was found to be 19775.31 with a pI of 5.36. The instability & the aliphatic indices of the protein were found to be 28.83 & 89.72 respectively. Both the instability and aliphatic index of the protein would indicate that the protein is a stable protein as observed in Bagchi (2020). The Grand Average of Hydropathy (GRAVY) score of the protein was found to be −0.378. This would indicate that the protein is non-polar.

3.2. The structural details of the screened ligands against Nsp1

The aforementioned structural and physico-chemical features of Nsp1 were used to screen the ChEMBL database and NCI database by the technique of virtual screening. We selected the top six ligands from the results of virtual screenings on the basis of their binding interaction energy values with Nsp1. However, the ligands screened from ChEMBL database were found to have better binding interaction energy values with Nsp1 as compared to the screened ligands from NCI database. Therefore, we used the screened ligands from ChEMBL database for further analyses. The structures of the selected ligand molecules were presented in Figure 3. The protein is mostly non-polar in nature. All the selected ligand molecules were found to have a stretch of hydrophobic carbon chains (Figure 3). An important aspect of any drug development endeavor is the identification of the ADME properties of the ligands. We calculated the ADME properties of the screened ligands and presented them in the Supplementary Table 1. Most of the selected ligands were found to possess requisite qualities as the potential antiviral drugs.

3.3. The binding interaction study of the selected ligand molecules with Nsp1

We generated the following Nsp1-ligand complexes:

1. Nsp1_CHEMBL1096281 (Ligand1)
2. Nsp1_CHEMBL2386944 (Ligand2)
3. Nsp1_CHEMBL1761178 (Ligand3)
4. Nsp1 _CHEMBL2022920 (Ligand4)
5. Nsp1_ CHEMBL464486 (Ligand5)
6. Nsp1 _CHEMBL175656 (Ligand6)

In order to study the behaviors of the Nsp1-ligand complexes in cellular environments, we performed MD simulations of the complexes as well as the free Nsp1 protein. We used the stable structure of Nsp1 obtained after MD simulation (section 2.1). We used the results of the MD simulation of free Nsp1 as the control. The progress of the MD simulation runs were analyzed by plotting the RMSD values of the Cα backbone atoms of the protein in free and ligand-bound states (Supplementary Figure 3) along-with the RMSF values of the amino acid residues of Nsp1 in free and ligand-bound states (Supplementary Figure 4). We also calculated the distance between the ligands and the two key amino acid residues, viz., Lys164 and His165 of Nsp1 apoprotein (Figure 4).

Finally, we computed the binding interaction energy values of the two key amino acid residues (Lys164 & His165 of Nsp1 apoprotein) with the ligands during the course of the MD simulations (Supplementary Figure 5) as these two amino acid residues are required by the Nsp1 apoprotein to bind to the 40S ribosomal subunit.

A stable binding of a ligand with a receptor can be determined by the structural deviation of the ligand. From the Supplementary Figure 3 we could identify that the ligands, viz., ligand1, ligand2, ligand4 and ligand6 (presented in gray colour) had comparatively lower structural fluctuations than the ligands, viz., ligand3 & ligand5. This would point towards the fact that the ligands, viz., ligand1, ligand2, ligand4, and ligand6 had stable conformations without any distortions in the relative dispositions of the functional groups present in them, which would be necessary to exert their functionalities as compared to the ligands, viz., ligand3 & ligand5. It was also observed from the Supplementary Figure 3 that all the Nsp1-ligand complexes became more stable than the Nsp1 apoprotein during the course of MD simulations. This would further reveal that in all the Nsp1-ligand complexes, the structural flexibility necessary for exerting the functionality of a protein was completely lost as Nsp1 was frozen to rigid conformation than the Nsp1 apoprotein,

From Figure 4 it was observed that the distances between the ligands and the key amino acid residues (Lys164 & His165) were gradually increased in cases of the ligands, viz., ligand2 & ligand3 (shown in orange and gray respectively). Therefore, it could be safely concluded that during the course of MD simulations the ligands, viz, ligand2 and ligand3 were getting drifted apart from the targeted key amino acid residues Lys164 & His165 of the Nsp1 protein. In short, these two ligands (ligand2 and ligand3) would have lower affinities towards the targeted key amino acid residues on the Nsp1 protein.

Furthermore, the analyses of the Supplementary Figure 4 would reveal that the rates of fluctuations of the two key amino acid residues (Lys164 & His165) of the Nsp1 protein were higher in cases of Nsp1-ligand2, Nsp1-ligand3 and Nsp1-ligand6 complexes in comparison to the Nsp1 apoprotein. The fluctuations were lower in cases of Nsp1-ligand1, Nsp1-ligand4 and Nsp1-ligand5 complexes in comparison to the Nsp1 apoprotein. Therefore, the ligands, viz., ligand2, ligand3 and ligand6 were not strongly bound to the key amino acid residues, Lys164 & Arg165, of the Nsp1 protein.

From Supplementary Figure 5 it was observed that the contributed binding interaction energy values of the two key amino acid residues (Lys164 & His165) were uniformly high

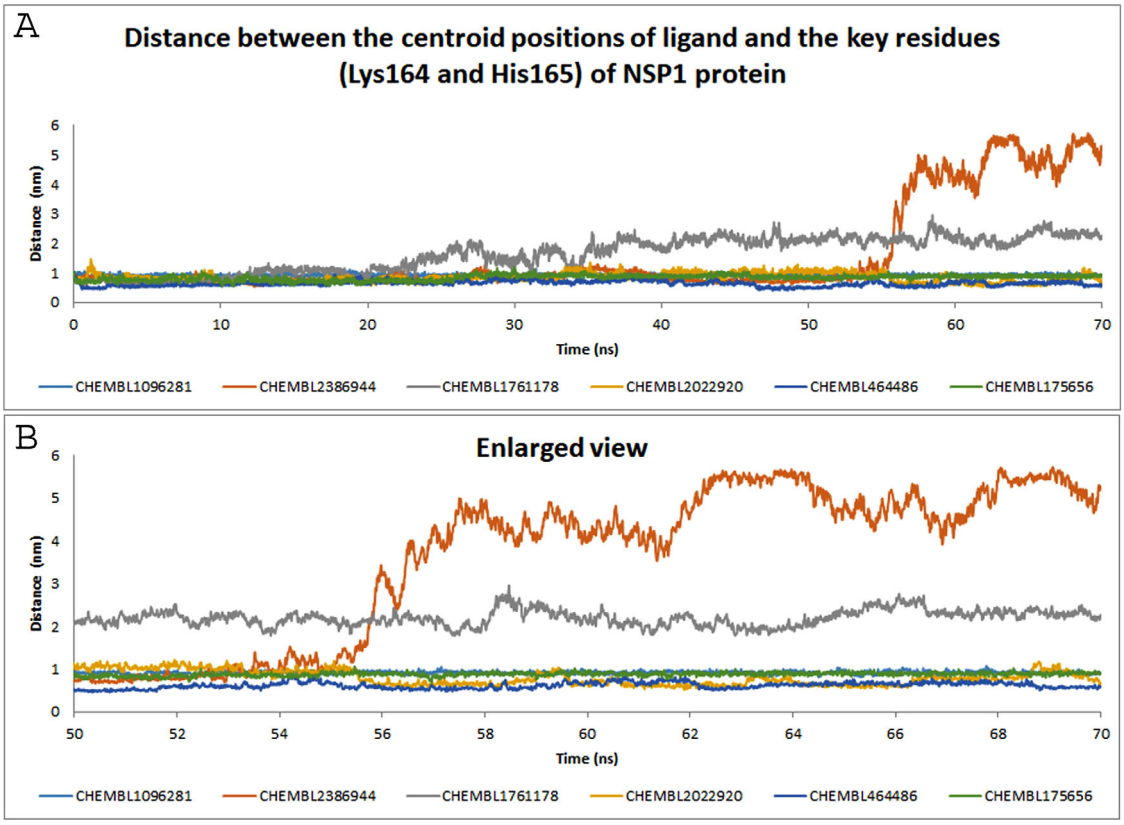

Figure 4. A. Distance between ligand and the key amino acid residues (Lys164 and His165) in the Nsp1 apoprotein. B. Enlarged view of last 20 ns of MD simulations.

in cases of Nsp1-ligand1 and Nsp1-ligand6 complexes throughout the MD simulation runs. In case of Nsp1-ligand5 complex, the binding interaction energy was found to be highly fluctuating. And in cases of Nsp1-ligand2, Nsp1-ligand3 & Nsp1-ligand4 complexes, the contributing binding interaction energy values of the two key amino acid residues, viz., Lys164 & His165 were found to be gradually changing into zero kcal/mol, during the course of MD simulation runs. These amino acid residues were found to be losing their contacts with the ligand2 and ligand3 during the course of MD simulations.

From the above observations, it could be concluded that the ligands, viz., ligand2 and ligand3 might not be suitable for targeting Nsp1 apoprotein as possible drug candidates as these ligands were found to be showing lower binding affinities towards the key amino acid residues of the Nsp1 protein.

The ligands, viz., ligand1, ligand4 & ligand6, were found to be bound to the key amino acid residues throughout the MD simulation runs. The energetics of the binding interactions between the protein and the ligands were presented in Table 1 which would clearly point towards the fact that the ligands, viz., ligand1, ligand4, and ligand6 could bind to the key amino acid residues more tightly than the ligand5. The positive binding interaction energy value of the ligand5 with the key amino acid residues of Nsp1 apoprotein would indicate not so favorable binding interactions between them.

Supplementary Figure 6 would indicate the extents of the different bond formations between Nsp1 apoprotein and the ligands during the MD simulation runs.

Supplementary Figure 7 would depict the structures of Nsp1 in free and ligand-bound states. These structures were obtained from the analyses of the MD simulation results. From these analyses, it was apparent that the ligands, ligand2 and ligand3, were found to be getting displaced from the target site.

Our analyses could clearly point towards the fact that the ligands, viz., ligand1 and ligand4, could bind both the key amino acid residues Lys164 and His165 very strongly as more numbers of intermolecular interactions had been being generated while ligand6 was able to interact only with His165 during the MD simulation run. However, among all the chosen ligands, the three ligands, viz., ligand1, ligand4 & ligand6 were found to be exhibiting strong binding interactions with the amino acid residues of Nsp1 apoprotein spanning the most important region 160 to 173, which is known to allow the virus to exert its function.

3.4. Computational alanine scanning of the residues Lys164 and His165

We performed computational alanine scanning (CAS) analysis of the two key amino acid residues (Lys164 and His165) of Nsp1. We used the protein ligand complex obtained from MD simulation, for the CAS analysis. For the CAS analysis we used Discovery Studio tool. The results are presented in Table 2.

From Table 2, it was revealed that the wild type Nsp1 could interact with the ligands in a better way than the

Table 1. MM/PBSA energy profile of top six NSP1-ligand complexes using bootstrap analysis.

NSP1_Ligand Complex	VDW Energy (kJ/mol)	Electrostatic Energy (kJ/mol)	Polar Solvation Energy (kJ/mol)	SASA Energy (kJ/mol)	Binding Energy (kJ/mol)
NSP1_CHEMBL175656	−135.408 (+/- 1.727)	−39.844 (+/- 1.723)	125.672 (+/- 3.372)	−13.968 (+/- 0.137)	−63.547 (+/- 2.084)
NSP1_CHEMBL1096281	−134.473 (+/- 1.740)	−12.628 (+/- 2.143)	110.338 (+/- 4.572)	−14.992 (+/- 0.157)	−51.587 (+/- 2.373)
NSP1_CHEMBL2386944	−22.290 (+/- 5.945)	−3.036 (+/- 1.089)	10.226 (+/- 8.813)	−3.158 (+/- 0.886)	−18.198 (+/- 6.435)
NSP1_CHEMBL1761178	−77.341 (+/- 4.942)	−9.325 (+/- 1.693)	56.343 (+/- 6.680)	−9.671 (+/- 0.547)	−40.251 (+/- 6.529)
NSP1_CHEMBL2022920	−96.993 (+/- 2.723)	−11.315 (+/- 1.843)	62.437 (+/- 3.031)	−11.594 (+/- 0.268)	−57.368 (+/- 3.077)
NSP1_CHEMBL464486	−144.436 (+/- 3.440)	76.817 (+/- 10.497)	225.491 (+/- 15.029)	−17.015 (+/- 0.386)	140.912 (+/- 5.683)

Table 2. Computational alanine scanning of the residues Lys164 and His165.

Protein-Ligand Complex	Binding Interaction Energy (kcal/mol) Wild Type	Binding Interaction Energy (kcal/mol) Mutant Lys164Ala	Binding Interaction Energy (kcal/mol) Mutant His165Ala
Nsp1_CHEMBL1096281	−34.85	−32.704	−25.392
Nsp1_CHEMBL2386944	−40.647	−25.18	−23.203
Nsp1_CHEMBL1761178	−27.405	−24.468	−23.109
Nsp1_CHEMBL2022920	−33.262	−20.778	−20.554
Nsp1_CHEMBL464486	−34.832	3.181	−0.127
Nsp1_CHEMBL175656	−42.728	−33.241	−30.981

mutants as reveled by the binding interaction energy values. In other words, the wild type Nsp1 had better binding affinities towards the ligands than the mutants. This would indicate the importance of the amino acid residues, Lys164 and His165, in ligand binding as mutations of these amino acid residues by alanine were found to lower the binding interactions of Nsp1 with the ligands.

3.5. Meta-analysis for the available data regarding SARS-Cov2 Nsp1

In order to collect and analyze the information on research going on using Nsp1 of SARS-Cov2 we performed a meta-analysis of the existing literature in PubMed literature database (https://www.ncbi.nlm.nih.gov/pubmed/) (Biswas et al., 2020). We used the following keywords while searching the database Nsp1, SARS-Cov2 Nsp1 ligand virtual screening, SARS-Cov2 Nsp1 drug repurposing, SARS-Cov2 Nsp1 molecular dynamic simulation. This was performed to get an overview on the published works on ligand screening against SARS-Cov2 Nsp1. We found that there are several works on the characterizations of SARS-Cov2 Nsp1 protein. In this work, our main focus was on the prediction of the structures of suitable ligands against Nsp1 and to analyze the real life behaviors of the ligands in the cellular environments. We have reported for the first time, about the impact of suitable antiviral compounds on the dynamics of Nsp1. We screened about 17,674 ligand molecules obtained from two different ligand databases. We measured the affinities of the different ligand molecules towards the Nsp1 from molecular dynamics aspect, where we found that some of the ligands would get detached from the active site of Nsp1 and some ligands would get attached strongly to the Nsp1 active site throughout the simulations.

4. Discussion

From the above analyses, it could be safely concluded that the ligands, viz., ligand1, ligand4 and ligand6 had the maximum binding affinities to the Nsp1 apoprotein. All these ligands could bind to the key amino acid residues, Lys164 and His165, which are vital to exert the activity of the Nsp1 apoprotein. The bindings of the ligand1 & ligand4 would also make the structure of the protein highly stable so that the protein would no longer be able to exert its regular activity. Above all, these ligands are proven anti-viral agents. Thus, the ligands may serve as potential inhibitors of Nsp1 from SARS-CoV-2. The activities of the ligands may therefore be tested in wet lab as potential therapeutic agents against the SARS-CoV-2. It is to be noted that till date most of the works pertaining to SARS-CoV-2 centered on the spike and the nucleocapsid protein (Calligari et al., 2020; Cava et al., 2020; Chen et al., 2020; Elfiky, 2020; Ibrahim et al., 2020; Tilocca et al., 2020). Our work is therefore unique in that sense. This work might be considered as providing insights into the preventative measures against the virus once it infects a human host.

Acknowledgements

The authors would like to thank UGC-SAP-DRSII and DST-PURSE-II and University of Kalyani for support.

Disclosure statement

No potential conflict of interest was reported by the authors.

References

Bagchi, A. (2020). Unusual nature of long non-coding RNAs coding for 'unusual peptides'. *Gene*, *729*, 144298. https://doi.org/10.1016/j.gene.2019

Berendsen, H. J. C., Grigera, J. R., & Straatsma, T. P. (1987). The missing term in effective pair potentials. *The Journal of Physical Chemistry*, *91*(24), 6269–6271. https://doi.org/10.1021/j100308a038

Biswas, S., Roy, R., Biswas, R., & Bagchi, A. (2020). Structural analysis of the effects of mutations in Ubl domain of Parkin leading to Parkinson's disease. *Gene*, *726*, 144186. https://doi.org/10.1016/j.gene.2019

Bodiwala, H. S., Sabde, S., Mitra, D., Bhutani, K. K., & Singh, I. P. (2011). Synthesis of 9-substituted derivatives of berberine as anti-HIV agents. *European Journal of Medicinal Chemistry, 46(4), 1045-1049*. https://doi.org/10.1016/j.ejmech.2011.01.016

Calligari, P., Bobone, S., Ricci, G., & Bocedi, A. (2020). Molecular investigation of SARS-CoV-2 proteins and their interactions with antiviral drugs. *Viruses*, *12*(4), 445. https://doi.org/10.3390/v12040445

Cava, C., Bertoli, G., & Castiglioni, I. (2020). Silico discovery of candidate drugs against Covid-19. *Viruses*, *12*(4), 404. https://doi.org/10.3390/v12040404

Chen Cao, Y., Xin Deng, Q., & Xue Dai, S. (2020). Remdesivir for severe acute respiratory syndrome coronavirus 2 causing COVID-19: An evaluation of the evidence. *Travel Medicine and Infectious Disease*, *35*, 101647. https://doi.org/10.1016/j.tmaid.2020.101647

Chen, Y. W., Yiu, C. B., & Wong, K. Y. (2020). Prediction of the SARS-CoV-2 (2019-nCoV) 3C-like protease (3CL pro) structure: Virtual screening reveals velpatasvir, ledipasvir, and other drug repurposing candidates. Version 2. *F1000Research*, *9*, 129. https://doi.org/10.12688/f1000research.22457.2

Cosconati, S., Forli, S., Perryman, A. L., Harris, R., Goodsell, D. S., & Olson, A. J. (2010). Virtual screening with AutoDock: Theory and practice. *Expert Opinion on Drug Discovery*, *5*(6), 597–607. https://doi.org/10.1517/17460441.2010.484460

De Tommasi, N., De Simone, F., Pizza, C., Mahmood, N., Moore, P. S., Conti, C., Orsi, N., & Stein, M. L. (1992). Constituents of *Eriobotrya japonica*. A study of their antiviral properties. *Journal of Natural Products*, *55*(8), 1067–1073. https://doi.org/10.1021/np50086a006

Eisenberg, D., Lüthy, R., & Bowie, J. U. (1997). VERIFY3D: Assessment of protein models with three-dimensional profiles. *Methods in Enzymology*, *277*, 396–406. https://doi.org/10.1016/S0076-6879(97)77022-8

Elfiky, A. A. (2020). Anti-HCV, nucleotide inhibitors, repurposing against COVID-19. *Life Sciences*, *248*, 117477. https://doi.org/10.1016/j.lfs.2020.117477 Epub 2020 Feb 28.

Fung, S. Y., Yuen, K. S., Ye, Z. W., Chan, C. P., & Jin, D. Y. (2020). A tug-of-war between severe acute respiratory syndrome coronavirus 2 and host antiviral defence: Lessons from other pathogenic viruses. *Emerging Microbes and Infections, 9, 558-570*. https://doi.org/10.1080/22221751.2020.1736644.

Gasteiger, E., Gattiker, A., Hoogland, C., Ivanyi, I., Appel, R. D., & Bairoch, A. (2003). ExPASy: The proteomics server for in-depth protein knowledge and analysis. *Nucleic Acids Research, 31, 3784–3788*. https://doi.org/10.1093/nar/gkg563

Gaulton, A., Hersey, A., Nowotka, M., Bento, A. P., Chambers, J., Mendez, D., Mutowo, P., Atkinson, F., Bellis, L. J., Cibrián-Uhalte, E., Davies, M., Dedman, N., Karlsson, A., Magariños, M. P., Overington, J. P., Papadatos, G., Smit, I., & Leach, A. R. (2017). The ChEMBL database in 2017. *Nucleic Acids Research*, *45*(D1), D945–D954. https://doi.org/10.1093/nar/gkw1074

Hess, B., Bekker, H., Berendsen, H. J. C., & Fraaije, J. G. E. M. (1997). LINCS: A linear constraint solver for molecular simulations. *Journal of Computational Chemistry*, *18*(12), 1463–1472. https://doi.org/10.1002/(SICI)1096-987X(199709)18:12<1463::AID-JCC4>3.0.CO;2-H

Ibrahim, I. M., Abdelmalek, D. H., Elshahat, M. E., & Elfiky, A. A. (2020). COVID-19 spike-host cell receptor GRP78 binding site prediction. *The Journal of Infection*, *80*(5), 554–562. https://doi.org/10.1016/j.jinf.2020.02.026

Jiménez-Alberto, A., Ribas-Aparicio, R. M., Aparicio-Ozores, G., & Castelán-Vega, J. A. (2020). Virtual screening of approved drugs as potential SARS-CoV-2 main protease inhibitors. *Computational Biology and Chemistry*, *88*, 107325. https://doi.org/10.1016/j.compbiolchem.2020.107325

Kamitani, W., Huang, C., Narayanan, K., Lokugamage, K. G., & Makino, S. (2009). A two-pronged strategy to suppress host protein synthesis by SARS coronavirus Nsp1 protein. *Nature Structural & Molecular Biology, 16, 1134–1140*. https://doi.org/10.1038/nsmb.1680

Kelley, L. A., Mezulis, S., Yates, C. M., Wass, M. N., & Sternberg, M. J. E. (2015). The Phyre2 web portal for protein modeling, prediction and analysis. *Nature Protocols, 10, 845-858*. https://doi.org/10.1038/nprot.2015.053

Laskowski, R. A., MacArthur, M. W., Moss, D. S., & Thornton, J. M. (1993). PROCHECK: A program to check the stereochemical quality of protein structures. *Journal of Applied Crystallography*, *26*(2), 283–291. https://doi.org/10.1107/S0021889892009944

Liang, J., Pitsillou, E., Karagiannis, C., Darmawan, K. K., Ng, K., Hung, A., & Karagiannis, T. C. (2020). Interaction of the prototypical α-ketoamide inhibitor with the SARS-CoV-2 main protease active site in silico: Molecular dynamic simulations highlight the stability of the ligand-protein complex. *Computational Biology and Chemistry*, *87*, 107292. https://doi.org/10.1016/j.compbiolchem.2020.107292

Mohamed, S. F., Flefel, E. M., Amr, A. E. G. E., & Abd El-Shafy, D. N. (2010). Anti-HSV-1 activity and mechanism of action of some new synthesized substituted pyrimidine, thiopyrimidine and thiazolopyrimidine derivatives. *European Journal of Medicinal Chemistry, 45, 1494-1501*. https://doi.org/10.1016/j.ejmech.2009.12.057

Narayanan, K., Huang, C., Lokugamage, K., Kamitani, W., Ikegami, T., Tseng, C.-T K., & Makino, S. (2008). Severe acute respiratory syndrome coronavirus nsp1 suppresses host gene expression, including that of type I interferon, in infected cells. *Journal of Virology*, *82*(9), 4471–4479. https://doi.org/10.1128/JVI.02472-07

Osorio, A. A., Munoz, A., Torres-Romero, D., Bedoya, L. M., Perestelo, N. R., Jimenez, I. A., Alcami, J., & Bazzocchi, I. L. (2012). Olean-18-ene triterpenoids from Celastraceae species inhibit HIV replication targeting NF-kB and Sp1 dependent transcription. *European Journal of Medicinal Chemistry*, *43*(38), no–no. https://doi.org/10.1016/j.ejmech.2012.03.035

Sagui, C., & Darden, T. A. (1999). Molecular dynamics simulations of biomolecules: Long-range electrostatic effects. *Annual Review of Biophysics and Biomolecular Structure*, *28*(1), 155–179. https://doi.org/10.1146/annurev.biophys

Sahin, A. R. (2020). 2019 Novel Coronavirus (COVID-19) outbreak: A review of the current literature. *Eurasian Journal of Medicine and Oncology, 4, 1-7*. https://doi.org/10.14744/ejmo.2020.12220

Shiryaev, S. A., Cheltsov, A. V., Gawlik, K., Ratnikov, B. I., & Strongin, A. Y. (2011). Virtual ligand screening of the national cancer institute (NCI) compound library leads to the allosteric inhibitory scaffolds of the West Nile virus NS3 proteinase. *Assay and Drug Development Technologies, 9, 69-78*. https://doi.org/10.1089/adt.2010.0309

Tilocca, B., Soggiu, A., Sanguinetti, M., Musella, V., Britti, D., Bonizzi, L., Urbani, A., & Roncada, P. (2020). Comparative computational analysis of SARS-CoV-2 nucleocapsid protein epitopes in taxonomically related coronaviruses. *Microbes and Infection*, *22*, 188–194. https://doi.org/10.1016/j.micinf.2020.04.002

Van Der Spoel, D., Lindahl, E., Hess, B., Groenhof, G., Mark, A. E., & Berendsen, H. J. C. (2005). GROMACS: Fast, flexible, and free. *Journal of Computational Chemistry*, *26*(16), 1701–1718. https://doi.org/10.1002/jcc.20291

Wiederstein, M., & Sippl, M. J. (2007). ProSA-web: Interactive web service for the recognition of errors in three-dimensional structures of proteins. *Nucleic Acids Research*, *35*(Web Server issue), W407-10. https://doi.org/10.1093/nar/gkm290

Wu, C. (2020). Analysis of therapeutic targets for SARS-CoV-2 and discovery of potential drugs by computational methods. *Acta Pharmaceutica Sinica B, 10, 766-788*. https://doi.org/10.1016/j.apsb.2020.02.008

Yeo, H., Li, Y., Fu, L., Zhu, J.-L., Gullen, E. A., Dutschman, G. E., Lee, Y., Chung, R., Huang, E.-S., Austin, D. J., & Cheng, Y.-C. (2005). Synthesis and antiviral activity of helioxanthin analogues. *Journal of Medicinal Chemistry*, *48*(2), 534–546. https://doi.org/10.1021/jm034265a

Yu, F., Wang, Q., Zhang, Z., Peng, Y., Qiu, Y., Shi, Y., Zheng, Y., Xiao, S., Wang, H., Huang, X., Zhu, L., Chen, K., Zhao, C., Zhang, C., Yu, M., Sun, D., Zhang, L., & Zhou, D. (2013). Development of oleanane-type triterpenes as a new class of HCV entry inhibitors. *Journal of Medicinal Chemistry*, *56*(11), 4300–4319. https://doi.org/10.1021/jm301910a